JTTEE5 25:143–159
DOI: 10.1007/s11666-015-0301-8
1059-9630/$19.00 © ASM International

Joining of Cast ZE41A Mg to Wrought 6061 Al by the Cold Spray Process and Friction Stir Welding

Victor Kenneth Champagne III, Michael K. West, M. Reza Rokni, Todd Curtis, Victor Champagne Jr., and Baillie McNally

(Submitted May 1, 2015; in revised form August 24, 2015)

This paper presents a novel method for joining cast ZE41A-T5 Mg to wrought 6061-T6 Al, without forming deleterious, coarse intermetallic compounds, which is not currently possible with conventional technologies. The novel aspect of the process includes the development of a joint design using cold spray (CS) as the enabling technology, to produce a transitional layer onto which a conventional welding technique can be employed to join the two dissimilar materials. The emphasis in this study will be on the CS transitional layer (T-layer) which enables the joining of cast ZE41A-T5 magnesium (Mg) and wrought 6061-T6 aluminum (Al) by friction-stir welding and the subsequent materials characterization to show the structural integrity of the entire joint. In order to join Mg and Al plates by this method, a transitional layer of CS Al is first deposited along the edge of cast ZE41A Mg plate. The CS Al T-layer enables the Mg to be friction stir welded to a plate of wrought 6061 Al, thereby completing the Mg plate to Al plate joint. Friction stir welding was chosen in this study to join the CS Al T-layer to the wrought Al plate; however, other conventional welding techniques could also be employed for joining Mg to Al in this manner. The CS Al T-layer is compatible to the wrought 6061 Al plate and serves as an insulating layer that prevents heat generated during the friction stir welding process from extending into the magnesium, thus preventing the formation of intermetallics. In this study, two sets of samples were produced joining cast ZE41A-T5 magnesium (Mg) and wrought 6061-T6 aluminum: one set using CS 6061 Al as the transition material between the ZE41A Mg plate and 6061 Al plate and the other set using CS 5056 Al as the transition material. Microstructural analysis by scanning and transmission electron microscopy and optical microscopy, along with mechanical test results including triple lug shear, tension, and micro hardness will be presented. Comparisons will be made to conventional joining techniques and the importance, as well as the applications of this technique, will be discussed.

Keywords cold spray, electron microscopy, mechanical properties, microhardness, microstructure, optical microscopy, tensile bond strength

1. Introduction

The ability to join magnesium and aluminum has been attempted using various welding processes such as diffusion (Ref 1, 2), friction stir (Ref 3), magnetic pulse (Ref 4), laser (Ref 5, 6), TIG (Ref 7), electron beam (Ref 8), and resistance spot welding (Ref 9) but with poor results. When aluminum (Al) alloys are welded to magnesium (Mg) alloys, the resulting welds are brittle due to the formation of an intermetallic layer at the dissimilar metal interface. It has been concluded by previous research that the formation of a large number of coarse Mg/Al intermetallic compounds cannot be avoided. These intermetallic layers can have a size magnitude of over 500-900 μm (Ref 11) and can cause cracking and brittleness in the welds, making them unsuitable for many applications. Cold metal transfer (CMT) dissimilar Al/Mg welding attempts have also been reported (Ref 10) but have resulted in poor mechanical properties and also brittle fracture of the intermetallic layer, at the dissimilar metal interface. The addition of a zinc alloy interlayer between Mg and Al during the diffusion bonding process has been found to significantly improve the microstructure of the bond zone at the interface, but deleterious coarse intermetallics are still formed in the bond region (Ref 1). Somasekharan and Murr (Ref 11) fabricated numerous welds from Mg alloys and the 6061-T6 Al alloy using friction-stir welding (FSW) with better results in that the formation of a large number of Mg/Al intermetallic compounds was avoided but not

This article is an invited paper selected from presentations at the 2015 International Thermal Spray Conference, held May 11-14, 2015, in Long Beach, California, USA, and has been expanded from the original presentation.

Victor Kenneth Champagne III, University of Massachusetts, Amherst, MA; **Michael K. West, M. Reza Rokni,** and **Todd Curtis**, South Dakota School of Mines and Technology, Rapid City, SD; **Victor Champagne Jr.**, U.S. Army Research Laboratory, Aberdeen, MD; and **Baillie McNally**, Worcester Polytechnic Institute, Worcester, MA. Contact e-mail: vchampagne@umass.edu.

altogether eliminated. In another study by Tomaa et al., the microstructure of the interface layer between Al (4043) and Mg (RZ5) joined by CMT was found to contain high concentrations of Al-Mg intermetallics (Al_3Mg_2 and $Al_{12}Mg_{17}$) (Ref 12).

2. The Cold Spray Process (CSP)

Cold spray is a material deposition process where combinations of metallic and non-metallic particles are consolidated to form a coating or near-net shaped part, by means of ballistic impingement upon a suitable substrate (Ref 13-15). The particles utilized are in the form of commercially available powders, typically ranging in size from 5 to 100 μm, that are typically accelerated to 300-1500 m/s by injection into a high velocity stream of gas. The high velocity gas stream is generated via the expansion of a pressurized, preheated, gas through a converging-diverging de Laval rocket nozzle. The pressurized gas is expanded to supersonic velocity, with an accompanying decrease in pressure and temperature (Ref 16-18). The particles, initially carried by a separate gas stream, are injected into the nozzle either prior to the throat of the nozzle or downstream of the throat. The particles are subsequently accelerated by the main nozzle gas flow and impacted onto a substrate after exiting the nozzle.

Upon impact, the solid particles deform and create mechanical and metallurgical bonds with the substrate (Ref 19, 20). Mechanical interlocking between impacting particles and the substrate occurs and is often compared to explosive bonding. Metallurgical bonding also takes place during impact as the kinetic energy of impacting particles is transformed into thermal energy. As the process continues, particles continue to impact the substrate and form both mechanical and metallurgical bonds with the consolidated material resulting in a uniform deposit with very little porosity and high bond strength. The term 'cold spray' has been used to describe this process due to the relatively low temperatures (−100 to 100 °C) of the expanded gas stream (Ref 21) and the low temperatures of the powder particles (~20 to 800 °C) (Ref 21) that exit the nozzle. The temperature of the gas stream is always below the melting point of the particulate material during cold spray, and the resultant consolidated material is formed in the solid state and the characteristics of the cold spray material are quite unique in many regards. The low temperatures associated with the cold spray process (CSP) are desirable, especially for joining dissimilar metals that have low melting points, such as aluminum to magnesium. The risk of grain growth and phase transformation is minimal or nonexistent, as is the formation of a heat affected zone (HAZ). Particle oxidation is avoided, as are tensile stresses that occur during thermal contraction, most often associated with welding techniques. Therefore, cold spray can be used in some instances to join dissimilar materials because the bond strength is equal to or greater than the ultimate tensile strength (UTS) of the weakest material being joined, as shown in this research.

3. Importance of Joining Dissimilar Materials

The ability to join dissimilar metals is a significant challenge for many industries, including the automotive and aerospace industries. The need for joining Al and Mg is to take advantage of the weight savings and subsequent energy efficiency in the automobile industry and the requirement for chemical plants and cryogenic applications. (Ref 22, 23) Dissimilar welding of aluminum (Al) and magnesium (Mg) alloys would achieve weight reduction and high efficiency of production by a substitution of Mg alloys for Al alloys. The military has dozens of applications in aerospace, munitions, and armored vehicles that require the joining of dissimilar materials including those associated with advanced armor. Reduction in weight and improvement of performance are important in the design and manufacture of armored military vehicles. These objectives must be accomplished without adversely affecting ballistic protection. Manufacturing methods to produce more efficient designs not only must be economically feasible, but also should rely on tools, materials, and skills readily available in the supplier community and be suited not only for production but also repair and for field use. In addition to joining dissimilar metals, in the form of conventional sheet, plate, or bar stock, there is a need to build-up dissimilar materials in more complex shapes to form tabs, flanges, protrusions, or even near-net parts. Cold spray can achieve these additional criteria.

The Welding Institute (TWI) published a review indicating that the need to join dissimilar materials is common to many industry sectors as customer demand is for products of enhanced performance, efficiency, increased quality, and reduced cost. (Ref 24) These industries include automotive, aircraft, farm equipment, petroleum, and natural gas. The automotive industry is implementing the use of dissimilar metals on subassemblies that hang on the vehicle frame. The automotive industry's target is to reduce car weight by taking out aluminum and steel components and replacing them with magnesium parts resulting in a weight reduction of 15% by 2020 in order to increase fuel efficiency by 9-12% (Ref 25). Car parts that are being switched out for magnesium parts are shock mounts that are attached to aluminum or steel frame rails and cross members which have been used on an aluminum subframe. Another dissimilar metals' application is the joining of steel substructures with aluminum skin panels on top: the steel provides the rigidity needed for crash safety and strength, and the aluminum provides corrosion resistance and reduces the total weight leading to better fuel efficiency (Ref 24). Another industry which requires the joining of dissimilar metals is the aerospace industry which has numerous propulsion, transmission, and airframe applications. Armored vehicles and tanks also require the joining of advanced aluminum and magnesium armor.

4. Experimental Procedure

4.1 Method to Join Plates of ZE41A-T5 Mg to 6061-T6 Al

Small rectangular plates measuring (10 cm × 4.5 cm × 0.64 cm thick) of cast ZE41A Mg and wrought 6061 Al were joined using a combination of cold spray and friction stir welding. First, the Mg plates were prepared in order to be suitable substrates for the CSP by grit blasting the edge that would be coated by the cold spray process, with a *Port-A-Blast* tool. This is a hand-held grit blasting unit and is used to remove oxides from the surface of the Mg allowing for better mechanical interlocking and metallurgical bonding of particles during cold spray. Metal to metal contact between incoming particles and the substrate are important for a superior bond. Next, a layer of CS Al was deposited on the edge of the Mg plate, using a prescribed proprietary robot path plan to maximize adhesion and strength. Proper control of the angle and working distance between the nozzle and the work piece were essential, as were other process parameters, which are listed in Table 1. The cold spray deposit formed the 'transitional layer' and is the key element of the joint design. If the T-layer was not adherent and structurally sound, then it would fracture from the Mg substrate during FSW. Two sets of samples were produced: one set with CS 6061 Al deposited onto ZE41A Mg and the other with CS 5056 Al deposited onto ZE41A Mg to form the T-layer, which was subsequently FSW to a plate of wrought 6061 Al. The final step of the joining process involved friction stir welding the cold spray transitional layer that had been deposited to the Mg plate to a wrought 6061 Al plate, thereby completing the joint between the ZE41A Mg and 6061 Al plate. Most of the materials' characterization work of the cold spray T-layer is dedicated to 6061 Al because the process development for 5056 Al was a recent discovery and occurred in the latter portion of this study, as part of another effort. However, the combination of high strength and ductility of the newly developed CS 5056 Al was significantly greater than that of CS 6061 Al and was included to provide another set of data to test the structural integrity of the entire joint in tension.

Table 1 CGT 4000 cold spray process parameters for the transitional layer

Feedstock powder
Powder: 6061 and 5056 Valimet -325 mesh and sieved by Vortec
Cold spray nozzle
Nozzle: Plastic type 33
Surface preparation
Materials to be joined: ZE41A-T5 Mg and 6061-T6 Al
Materials surface preparation: Grit Blast using 'virgin' 60 Grit @ 0.7 MPa
Materials Surface Cleaning: Ethanol + Air
Cold spray process
Gas type: He
Gas mode: pressure
Gas pressure: 2.8 MPa
Heater: 400 °C Gun, 300 °C Pre-heat
Powder feeder: 12 g/min
Measured: powder feeder RPM = 1.1, main gas flow = 143
Robot program: raster
Stand off: 25 mm
Raster speed: 600 mm/s

4.2 Summary of Technical Approach

1. Clean and grit blast one edge of a Cast ZE41A-T5 Mg plate.
   - (4) Samples each 10 cm long, 4.5 cm wide and 0.64 cm thick.
2. Cold Spray 6061 & later 5056 Al onto the prepared edge of the Cast ZE41A-T5 plate to form the T-layer.
   - Sufficient in thickness to accommodate a FSW weld (~1.5 cm).
   - Finish machine to blend with Mg plate.
3. Clamp a 0.6 cm wrought 6061-T6 Al plate to the cold spray Al T-layer of the Mg.
4. Friction Stir Weld the wrought 6061-T6 Al plate to the cold spray Al T-layer deposited onto the ZE41A-T5 Mg.
5. Prepare shear, tensile, and metallographic specimens for mechanical testing & optical and electron microscopy.
6. Compare results to conventional welding techniques.

4.3 Mechanical and Microstructural Evaluation of Materials

The structural integrity of the CS 6061 Al/ZE41A Mg bond or 'T-layer' was examined using the triple lug shear test. This test was chosen because it provides a means of measuring the strength of the cold spray bond beyond the limits of the conventional adhesion test ASTM C633, ''Standard Test Method for Adhesion or Cohesion Strength of Thermal Spray Coatings.'' The ASTM C633 relies on the strength of an epoxy adhesive, which is normally not much higher than 70-80 MPa (Ref 26). Cold spray coatings can achieve much higher bond strengths, and therefore, the Triple Lug Shear Test performed according to military specification, MIL-J-24445A, was employed to obtain a quantitative measure of the shear strength of the cold spray T-layer. The Al/Mg interface was then analyzed with optical and scanning electron microscopy. The tensile strength of the 6061 Al and 5056 Al cold spray material used to produce the transitional layer was tested alone by producing two separate blocks of these materials approximately 12 cm × 12 cm × 1.3 cm thick and subsequently machining tensile coupons from them to compare to that of wrought 6061-T6 Al. Tensile and hardness testing, as well as optical and electron microscopy of the entire joint were conducted. TEM was also conducted at the interface of the cold spray aluminum transitional layer and the magnesium substrate to determine if any intermetallics were formed. The FSW process was confined to a region encompassing the wrought 6061 Al substrate and the cold spray aluminum transitional

layer, preventing the formation of Mg/Al intermetallics, because the T-layer acted as a thermal insulator and a barrier to prevent diffusion.

5. Cold Spray Processing (CSP)

Two sets of samples were fabricated: one set with CS 6061 Al and the other with CS 5056 Al to form the transitional layer enabling FSW to be performed to join the Mg plate to the Al plate without forming coarse intermetallic compounds.

5.1 Feedstock Powder for Cold Spray

The 6061 Al powder was gas atomized and procured from Valimet, Inc., Stockton CA. The specified particle size cut was -325 mesh which corresponds to a maximum particle size of approximately 44 μm. The 6061 powder provides an advantage over pure aluminum in terms of hardness and strength and was used to join ZE41A-T5 Mg to 6061-T6 Al. Particle size and morphology were confirmed using a Horiba LA-910 Laser Scattering Particle Size Distribution Analyzer and an Environmental Scanning Electron Microscope (ESEM). A particle size distribution for the 6061 Al is provided in Fig. 1. The Specific Surface Area was 5331.4/cm and is defined as the total sum of the surface area of the sample particle per unit volume. The specific surface area is calculated on the assumption that the surface of the particle is a smooth globular shape. The Mean Particle Size was 27.9619 μm. Figure 2 shows that the 6061 Al particles were generally spherical in shape. The powder contained a mixture of larger and smaller particles, as well as a limited number of micro-satellite-sized particles (i.e., <5 μm). Excessive fine particles can cause problems during the cold spray operation by clogging the nozzle and should be reduced to a minimum through powder classification.

5.2 Surface Preparation of ZE41A-T5 Mg plates

The surface preparation used for all the ZE41A-T5 magnesium substrates was an abrasive blast followed by a solvent rinse of ethanol. The abrasive blast equipment was a *Port-A-Blast* which is used to grit blast the surface of the substrate to remove oxides in preparation for cold spraying. This equipment does not recycle the abrasive. The use of uncontaminated abrasive was necessary to minimize the embedding of corrosive materials such as iron into the magnesium substrate. This can occur if the oxide particles fragment and become angular with continued use. The abrasive media used was a 60 grit aluminum oxide. This media was sprayed at 0.7 MPa pressure at a 45° stand-off angle. The stand-off distance was 10-15 cm away from the surface of the part.

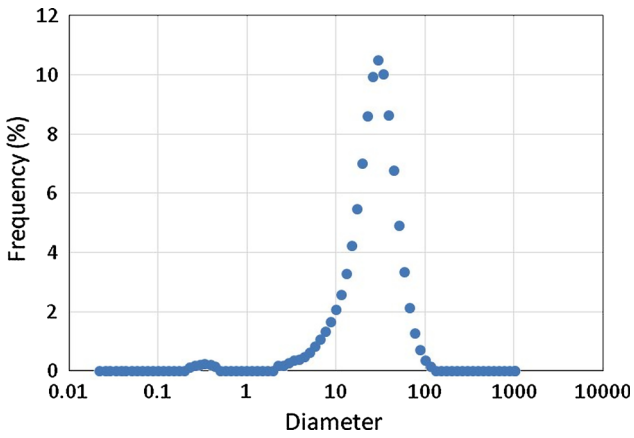

Fig. 1 Particle size distribution for Valimet -325 mesh 6061 aluminum alloy

5.3 Cold Spray Equipment and Process Parameters

Cold spray aluminum was deposited on the grit blasted magnesium to act as a transition layer in order to join the two metals (see Fig. 3). The CGT 4000-47 kW system was utilized in this study. It has two gas heaters (30 kW which is on the floor and a 17 kW heater on the gun) as shown in Fig. 4. It can attain temperatures of accelerating gas up to 800 °C and corresponding gas pressures up to 4 MPa. The cold spray gun is controlled by a 6-axis Fanuc robot. Robot path planning is used to control the precise angle, traverse speed, and working distance of the spray nozzle to the substrate.

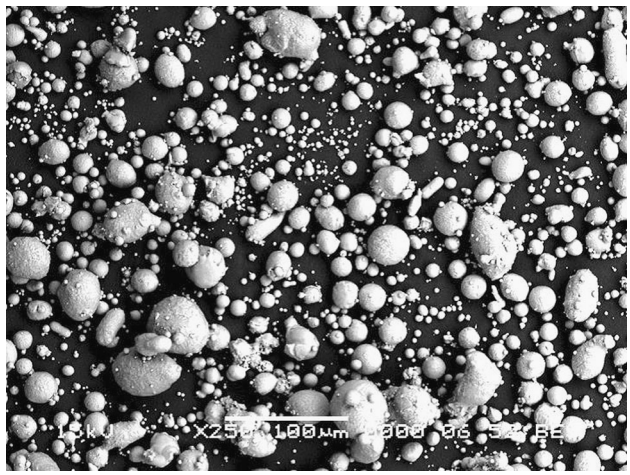

Fig. 2 ESEM Micrograph of Valimet -325 mesh 6061 aluminum alloy powder

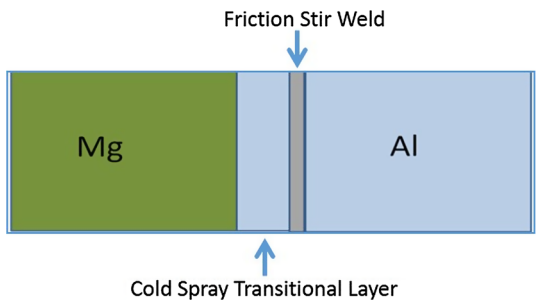

Fig. 3 A schematic of how the samples were prepared to enable cast ZE41A Mg to be joined to wrought 6061 Al by a combination of the cold spray process and friction-stir welding is shown

The control of gas pressure and temperature is important during the cold spray process. Particle velocities and temperatures are two of the key variables in the CSP that affect deposition rate and efficiency. Modeling these variables eliminates iterative and extraneous experimentation. Input variables include but are not limited to nozzle geometry, carrier gas type, particle density, gas viscosity, operating pressure, gas temperatures, and particle size. Particle temperature and particle velocity at the substrate are two of the variables which are modeled. The modeling program also provides estimates for deposition efficiency, as well as coating cost per area. Both of these estimates are extremely practical tools which aid implementation of cold spray technology but are beyond the scope of this paper to discuss in detail.

The modeling of impact velocity and deposition efficiency can be broken down into following specific areas:

- The gas flow and temperature in the nozzle are calculated by means of isentropic (frictionless) gas dynamic principles and empirically measured by a DPV 2000 laser-based particle velocity measuring system.
- Drag and heat transfer coefficients from solid rocket analyses are used to iteratively calculate particle velocity and temperature through the nozzle to determine the ''critical impact velocity'' (CIV).
- An empirical relationship between the particle velocity and particle material characteristics is used to calculate the deposition efficiency or the percent of incoming particles that adhere and form a well-bonded deposit, which in turn is used to determine the optimal CSP parameters that will result in adequate consolidation.

Fig. 4 CGT 4000 high-pressure cold spray system used to produce the transitional layer

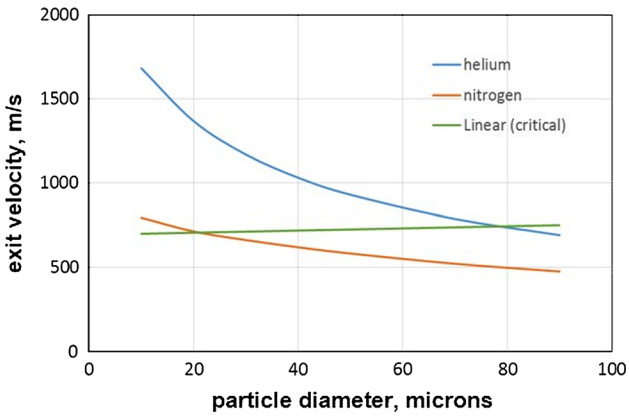

Fig. 5 Plot of particle exit velocity of 6061 Al comparing helium and nitrogen carrier gases at 400 °C, 30 bar with critical impact velocity shown

The particle velocity in cold spray is modeled by taking into account gas type, pressure at the nozzle throat, and nozzle dimensions, such as the throat diameter, nozzle length, and exit diameter. Particle velocities modeled as a function of particle size are shown in Fig. 5, which represent the particle exit velocity of 6061 Al comparing helium and nitrogen as the accelerating gases at 400 °C, 30 bar. The plot also shows the CIV for 6061 Al, which is defined as the minimum velocity required for adequate consolidation of the impacting particles.

The difference in particle velocities between He and N_2 is quite significant, and the decision to choose helium as the accelerating gas for 6061 Al particles with a mean particle size of 28 μm is quite apparent. Particles <20 μm would have less than adequate consolidation and would form consolidated material with significant levels of porosity and be weak and brittle in nature.

A spray nozzle fabricated from PolyBenzImidazole (PBI) was used to cold spray the 6061 and 5056 aluminum. Standard tungsten carbide nozzles experience clogging when aluminum powders are used. The PBI is a high-performance-imidized thermoplastic capable of withstanding high temperatures while retaining mechanical properties without melting and has been in use for over 10 years as the preferred material for cold spraying aluminum. PBI also has superior wear resistance at elevated temperatures (such as those used to cold spray aluminum) than other reinforced engineering plastics. Table 1 lists the CSP parameters used for both the 6061 Al and 5056 Al transitional layer. Other parameters such as robot raster speed, nozzle material, and stand-off distance were optimized for 6061 and 5056 aluminum coatings for the study.

5.4 Friction Stir Welding Process

Friction Stir-welding was chosen to join a plate of cast ZE41A-T5 Mg that contained a 6061 CS T-layer on one edge to a plate of wrought 6061-T6 Al. The purpose of the cold spray transitional material was to mitigate the formation of a deleterious intermetallic layer at the dissimilar metal interface. The cold spray T-layer served as an insulator and minimized thermal energy from the FSW. FSW also allows for minimal heat transfer across the cold spray layer.

The process parameters used to stir weld the plates together were 800 RPM, 10 IPM, a 1° Lead Angle, and a 0.15 IPM Plunge Rate. The two plates to be joined were

initially machined to ~3.6-mm thickness and a pin length 3.3 mm. The pin tool details are shown in Table 2, and a photo of the pin tool is shown in Fig. 6. It is important to note that the temperature of the FSW approximates 80% of the melting point of the Al. Figure 7(a) shows the plates clamped to the FSW fixture with the rotating pin plunged into the CS T-layer and the wrought 6061-T6 Al joining it to the ZE41A-T5 Mg. Figure 7(b) shows the finished FSW joint. The cold spray T-layer remained intact, and the dissimilar metals were successfully joined together.

Table 2 Pin tool details

Two piece adjustable pin tool
10.8 mm diameter shoulder—concave
10° tapered pin with 3 flats
Material Type—H13 tool steel shoulder with MP159 Pin

Fig. 6 FSW Tool fabricated from H13 tool steel with a MP159 pin

5.5 Triple Lug Shear Strength Test

The Triple Lug Shear Test (TLST) method was used to study the adhesive shear behavior of the cold spray transitional layer (6061 Al cold sprayed onto ZE41A-T5 magnesium). This test was chosen to determine the structural integrity of the T-layer and whether it would be sufficient to withstand the friction stir welding process. The TLST would provide a quantitative measure of shear strength and was originally intended for bimetallic joints for welded structures, where steel is bonded to aluminum alloys by roll bonding and explosive bonding processes (Ref 27). The triple lug procedure method is prescribed in military specification, MIL-J-24445A. A schematic of the TLST specimen is shown in Fig. 8(a). A deposit with a thickness of greater than 0.3 mm is applied onto a plate of ZE41A-T5 Mg by the cold spray process. Three rectangular-shaped 'lugs' are machined from the 6061 Al cold spray material (Fig. 8b). The lugs are then sheared from the test specimen using a compressive load frame setup (Fig. 9). Only one lug is sheared from the specimen at a time. Failure stress is reported based on the load at failure and the surface area of the lug. Control specimens milled from single pieces of cast ZE41A Mg were included in the matrix to establish a baseline for comparison. Four samples having three lugs/sample for a total of 12 data points from each of the two groups were tested in shear in a universal tensile testing machine (MTS, Systems Corporation, Eden Prairie, MN) under displacement control at constant cross-head speed of 1 mm/min. The applied load was measured continuously with a 25 kN load cell. The force required to shear off the coating and the coating/substrate attachment area then yielded the shear strength of the bond. All of the 6061 Al cold spray lugs showed very high adhesion on the magnesium alloy.

The average adhesive strength of the 6061 Al cold spray lugs on ZE41A-T5 Mg was about 140.7 MPa and exceeded the average strength of the base line ZE41A-T5 Mg substrate samples, which was 122 MPa (Table 3). The 6061 Al cold spray lugs on the ZE41A-T5 broke off by fracturing material well beneath the Al/Mg interface.

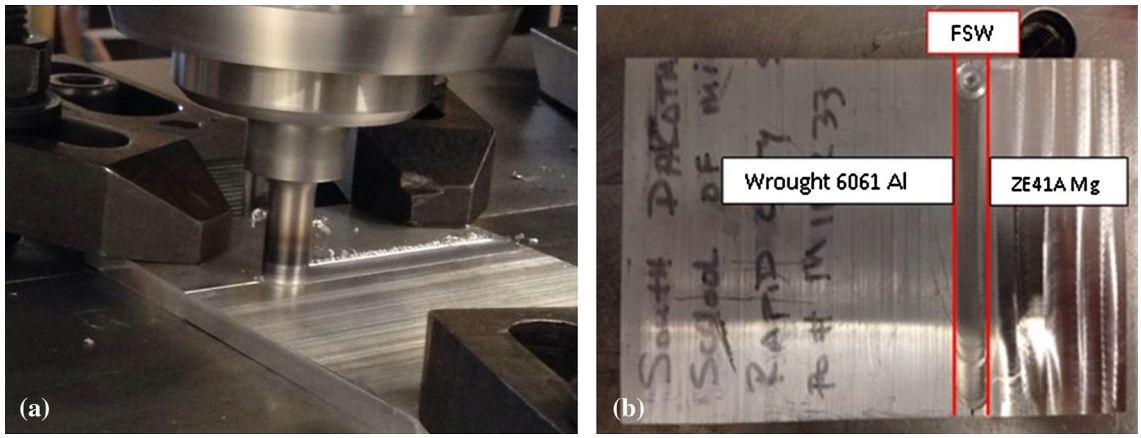

Fig. 7 (a) Friction Stir Welding setup and in progress showing the rotating pin plunged into the CS T-layer and the wrought 6061-T6 Al joining it to ZE41A-T5 Mg (b) FSW sample of wrought 6061-T6 Al joined to ZE41A-T5 Mg

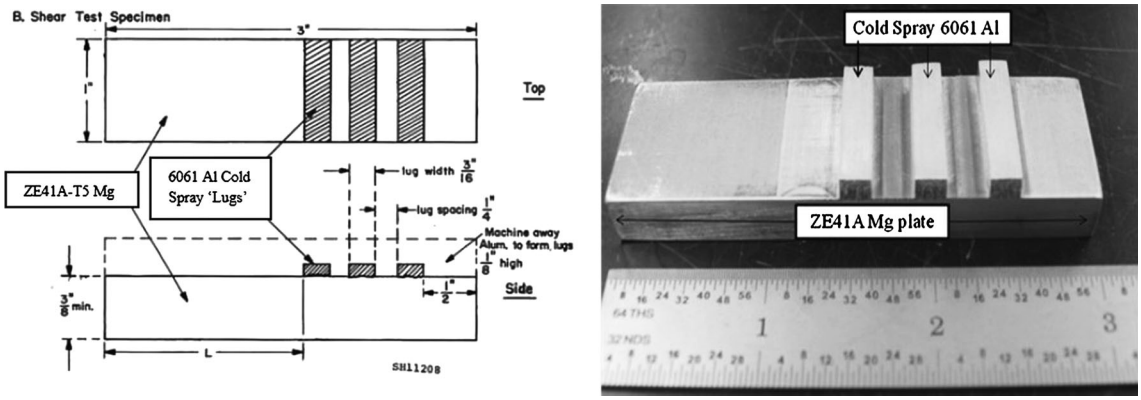

Fig. 8 Schematic of the MIL-J-24445A triple lug shear test specimen alongside an actual sample (Ref 28)

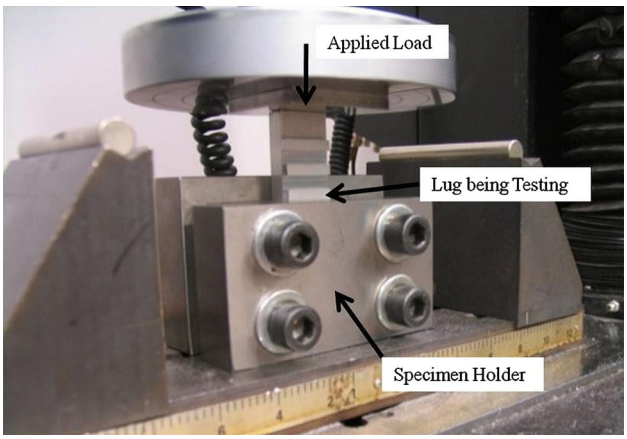

Fig. 9 Triple Lug Shear Test setup in a universal tensile testing machine

This provides a positive indication that the strength of the bond between ZE41A-T5 Mg and the CS 6061 Al T-layer is sufficient to enable FSW, since the weakest point is not the CS 6061 Al T-layer.

5.6 Microstructural Analysis of the Cold Spray Transitional Layer

The microstructural features of the cast ZE41A-T5 Mg samples coated with 6061 Al by cold spray in preparation for FSW, as shown in Fig. 10, were evaluated by optical microscopy and scanning electron microscopy (Supra-40, Zeiss, Oberkochen, Germany). Cross sections of the edge were taken utilizing a LECO cut-off saw, and one-inch diameter metallographic samples were mounted in Bakelite and prepared incorporating a series of grinding steps starting at 180 grit and finishing with 2400 grit. Final polishing was accomplished using 3 μm diamond paste followed by ¼ μm diamond paste and completed using a 0.05 μm colloidal silica suspension. The important aspect of the evaluation was that, as anticipated, no evidence of a

Table 3 Triple lug shear test results

Material (12 data points each)	Average max load, MPa	Std. deviation, MPa	95% Confidence interval, MPa
Cast ZE41A-T5 Mg	122.0	7.6	4.1
6061 cold spray on ZE41A-T5 Mg	140.7	5.5	2.8

HAZ was observed, since the CSP was accomplished below any phase transformation temperatures and well below the melting point of both materials (Fig. 10a, b). Figure 10(a) represents an as-polished sample showing the interface of the cast ZE41A-T5 Mg and the cold spray 6061 Al T-layer taken with the scanning electron microscope (SEM). The interface showed no inherent defects such as porosity, cracks, oxide inclusions, or coarse intermetallic compounds. Grain boundary β-Mg-Zn-RE phase was present and is described further in Fig. 11. The CSP layer near the substrate interface had a good deposition quality with no obvious evidence of porosity, triple junction voids, and lack of bonding between powder particles. This demonstrates suitable local particle deformation due to proper selection of CSP parameters. Figure 10(b) shows the same area but using optical microscopy and after being etched with Keller's reagent. Figure 10(b) shows no coarse intermetallic formation at the interface. Transmission electron microscopy was also performed to confirm these findings.

Figure 10(b) illustrates the tremendous plastic deformation that occurs between the high velocity impacts of the spray particles resulting in very high strain rates. Upon impact, the plastic deformation disrupts and breaks down surface oxide layers on both the powder and substrate leading to a metallurgical bond, as well as mechanical interlocking. Since the feedstock powder is deposited in the solid state, the microstructure is retained after deposition with the exception of dynamic recrystallization due to high strain levels. Localized temperature increases, and strain concentration plays a major role in the high-speed

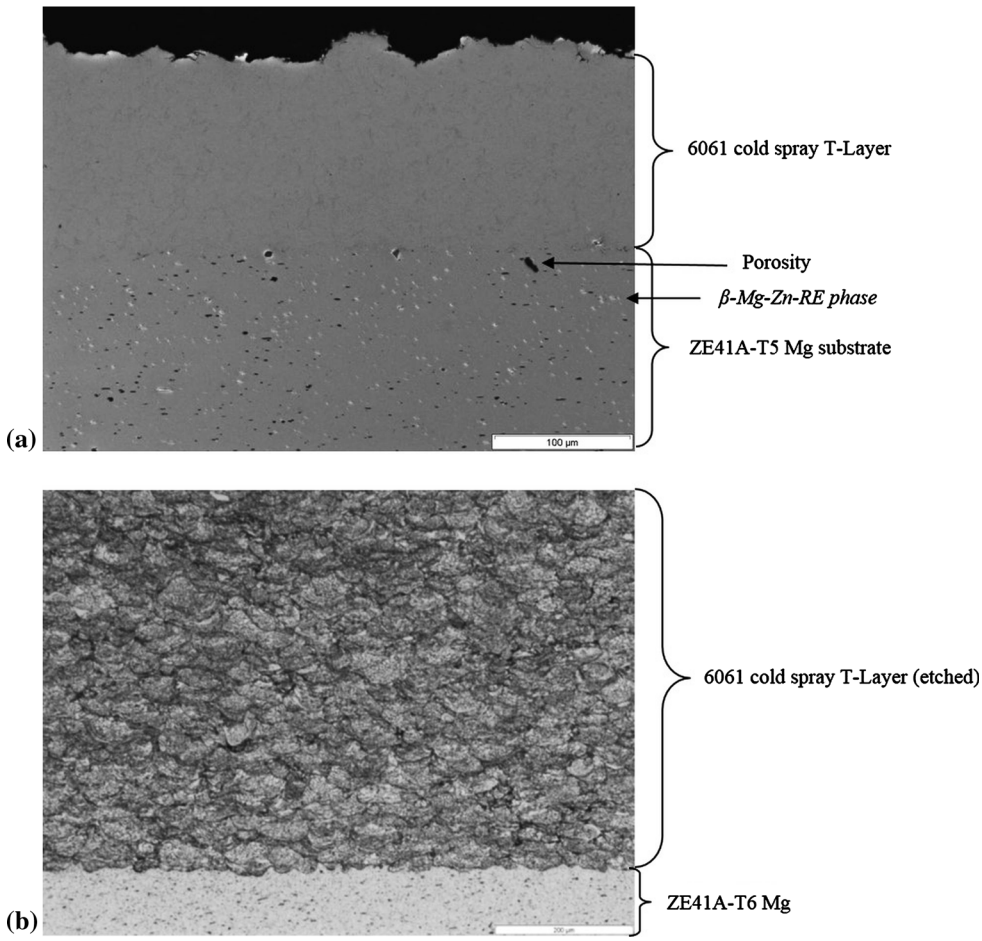

Fig. 10 (a) Scanning electron microscope image of an as-polished cross-section of the 6061 Al/ZE41A-T5 Mg interface (b) Etched microstructure of 6061 Al deposited onto ZE41A-T5 Mg

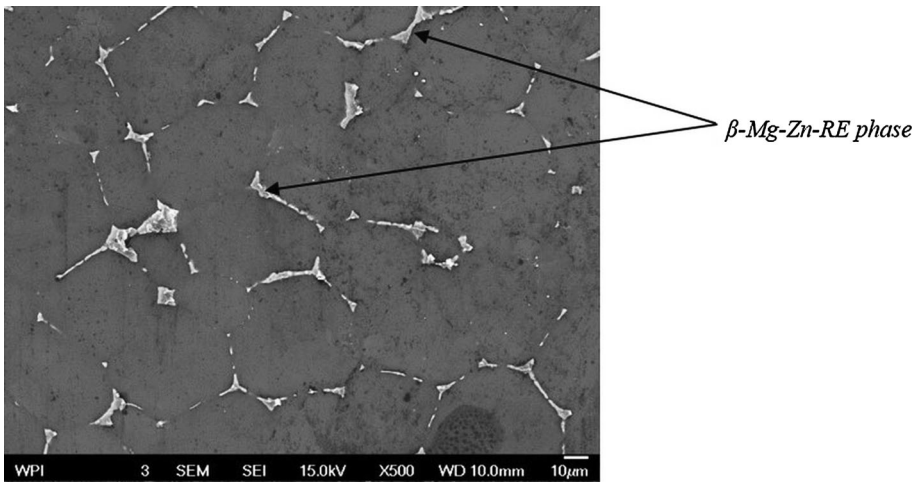

Fig. 11 SEM of the ZE41A-T5 Mg substrate showing grain boundary β-Mg-Zn-RE phase

deformation of the aluminum particles upon impact resulting in adiabatic shear. The large number of particles in flight can cause interactions between particles either before or even during impact. Finally, deposited highly strained particles may be impacted immediately by other particles straight away following the deposition of the next

layer of impacting particles. This limited relaxation time after the deposition, in turn, can cause high-strain hardening (Ref 28).

The magnesium alloy ZE41A is a casting alloy having a combination of light weight, stiffness, and high strength and is currently used in the military and commercial aerospace industry for applications as high as 250 °C for transmission housings. Figure 10(a) shows some evidence of porosity that is expected from a sand casting. These defects lower the ductility of the Mg and serve as stress concentration regions. The major alloying elements are Zn and Zr, as well as the rare earth element cerium as shown in Table 4 (Ref 29). This alloy has a thermally stable microstructure consisting of an α-Mg matrix, Mg eutectics, and various primary and secondary phases containing rare earth elements (Ref 30). The ZE41A Mg cast alloy is heat treated to the T-5 condition, which is an artificially aged condition and the microstructure consists of α-Mg and β-Mg-Zn-RE according to Riddle et al. (Ref 31). Figure 11 is an SEM image at high magnification depicting the β-Mg-Zn-RE grain boundary phase. Cerium is the rare earth alloying element for ZE41A and has a positive effect on creep resistance after aging. Additional precipitates form within the grains and at the grain boundary that reduce grain boundary sliding (Ref 32).

Table 4 Chemical composition of ZE41A magnesium (Ref 29)

Elements	wt.%
Cerium, Ce	0.75-1.75
Copper, Cu	≤ 0.10
Magnesium, Mg	94
Manganese, Mn	≤ 0.15
Nickel, Ni	≤ 0.010
Zinc, Zn	3.5-5.0
Zirconium, Zr	0.40-1.0

Zirconium is used to refine grain size and zinc serves as a strengthening alloy being found in solid solution and associated with the grain boundary precipitates as shown in Fig. 11.

Figure 12 depicts the adherent bond observed between the CS 6061 Al T-layer and the ZE41A Mg. The micrographs clearly show that the deposit has completely attached and welded to the substrate as there was no evidence of porosity or lack of bonding observed along the interface. This observation demonstrates adequate local particle deformation due to proper determination of high-pressure cold spray deposition parameters.

Figure 13(a) shows an enlargement of the highly deformed particles. In the Z direction, the grain structure is deformed normal to the impact direction and is elongated, while in the Y direction, the material has been compacted between layers of impacting particles, resulting in a compression of the grain structure, analogous to a stack of playing cards. There are instances of triple junction voids (Fig. 13a, b) in the deposited layer, which may cause lower ductility in the Z direction (Ref 33). These voids generally form because of the lack of local deformation in the particles caused by the nature of the coating process (Ref 34). The main reason for the presence of these occasional voids in the microstructure of the Z direction can be related to the CIV. The CIV can be defined as the velocity at which adequate consolidation of the particles is achieved based upon the amount of plastic deformation and can be determined by predictive models (Ref 35). Larger particles carried in the gas stream may not be able to achieve the CIV, and would experience limited deformation during impact as shown in Fig. 13(a). Particle velocity is also influenced by the location of the particles in the gas stream and the degree of randomness in both the particle acceleration kinetics and the particle and substrate interaction, i.e., the variations in the substrate geometries as the deposition builds up (Ref 33).

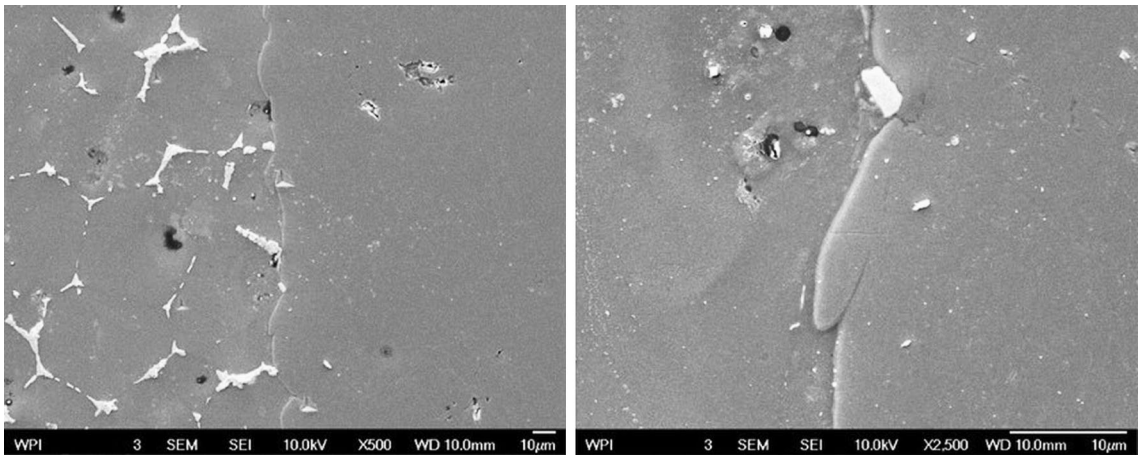

Fig. 12 SEM of the 6061Al CS T-layer at the ZE41A Mg interface

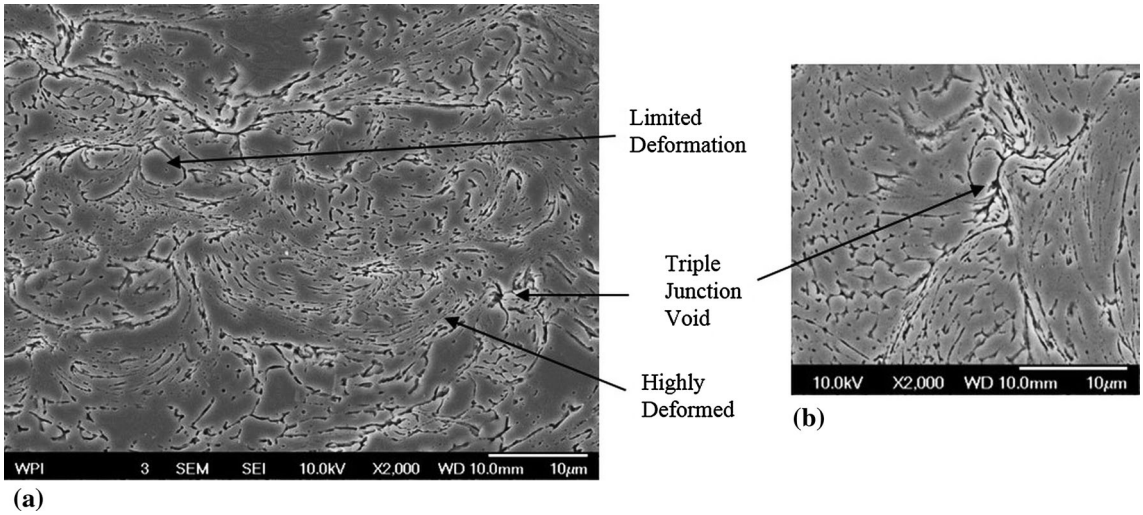

Fig. 13 (a) and (b) SEM of CS 6061 T-layer showing varying degrees of plastic deformation and consolidation

Table 5 Tension test results of cold spray 6061 Al compared to wrought 6061 Al. (Ref 36)

6061 Condition	UTS, MPa	YS, MPa	%EL
T6 (Ref 37)	310	276	12
CS sample 1	319	270	4.43
CS sample 2	314	247	4.96
CS sample 3	316	252	6.40
CS sample 4	310	237	5.18
CS (average)	315	252	5.2

5.7 Tension Testing of the 6061 Al Cold Spray Material Comprising the Transitional Layer

A total of 6 tensile bars were cut from CS 6061 Al deposited to form blocks of material approximately 12 cm × 12 cm × 1.3 cm thick. The yield strength (YS) and the UTS of the cold spray 6061 Al are listed in Table 5. The tensile test results showed that the CS 6061 Al has a very high strength (315 MPa), in the as-cold sprayed condition. The primary strengthening mechanism is the work hardening that occurs during particle impact and consolidation in the solid state. The elongation at failure (%EL) is ~5%, which exceeds that of the ZE41A-T5 Mg, which is about 3%. Tension data from a newly developed CSP for 5056 Al were generated toward the end of this study as part of another related effort and was incorporated because of the tremendous combination of high strength and high ductility. Tensile test results indicated that by varying, the temperature and pressure during the cold spray process, combinations of UTS (400 MPa) and elongation (15-22%) could be achieved. Therefore, a decision was made to take advantage of these unique properties and use a 5056 Al CS T-layer to produce a special set of samples specifically for tensile testing the entire joint, which is included in the FSW analysis section.

5.8 Microstructural Examination of the FSW Samples

Figure 14 shows a cross section of the completed welded joint in the etched condition, as observed optically. These images are a montage of the various zones of the welded joint: the entire image would be much larger than what is shown; therefore, representative images were taken at the most important regions, including the interfaces of the plates being joined and the cold spray 6061 Al Transitional layer.

The cold spray material served as the transitional material allowing the two dissimilar metals to be joined without any formation of undesirable intermetallics or other undesirable microstructural features, such as HAZs or the formation of an as-cast structure. The blended material associated with the FSW areas can easily be discerned from the base wrought 6061 Al and 6061 CS T-layer. Evidence of an intercalated microstructure with vortexes associated with FSW, as a result of mechanical mixing of the two metals was observed, also reported by Somasekharan and Murr (Ref 11). Even at the relatively low magnification, the fine grains of the CS 6061Al transitional layer can be seen in contrast to the disrupted grain pattern within the FSW zone. The sample was etched with Kellers reagent for 20 s.

Figure 15(a) shows the interface region between the wrought 6061 Al and the FSW nugget. The gray microstructural features within the wrought 6061 Al are particles of Fe_3SiAl_{12}, while the black features are Mg_2Si precipitates. During the FSW process, the thermo-mechanically affected zone is where the material undergoes heavy plastic deformation. The heat generated between the non-consumable pin and the adjacent material not only allows plastic deformation to take place but can also affect the microstructure and the resultant material properties, such as hardness. Figure 15(b) shows coarsening of the precipitates and overaging can occur which would lower the hardness and strength of the 6061 Al.

In the CS 6061 Al T-layer (Fig. 15c), localized temperature increases, and strain concentration plays a major role in the high-speed deformation of the aluminum particles upon impact causing adiabatic shear. Much of the work of plastic deformation is converted to heat, and the

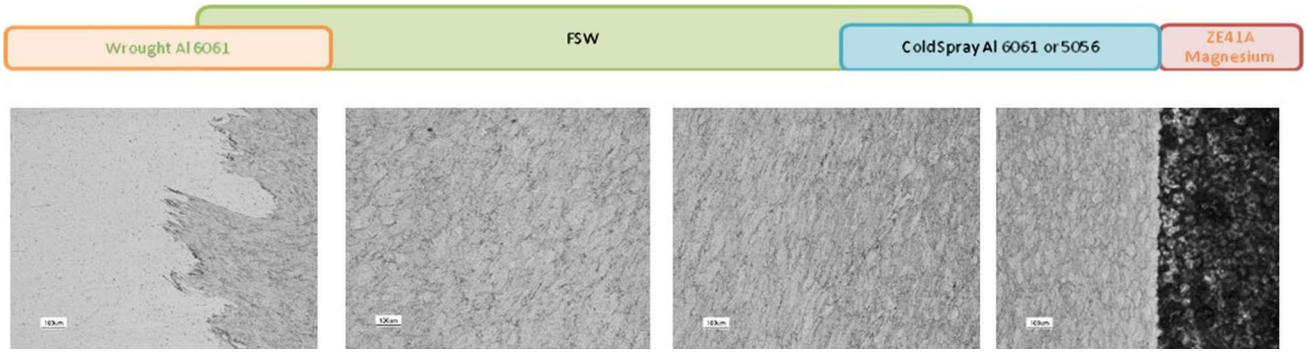

Fig. 14 Montage of a cross section of the completed welded joint showing the wrought 6061 Al, the FSW, the CS 6061 Al Transitional layer and the cast ZE41A Mg in the etched condition. Each marker represents 100 μm

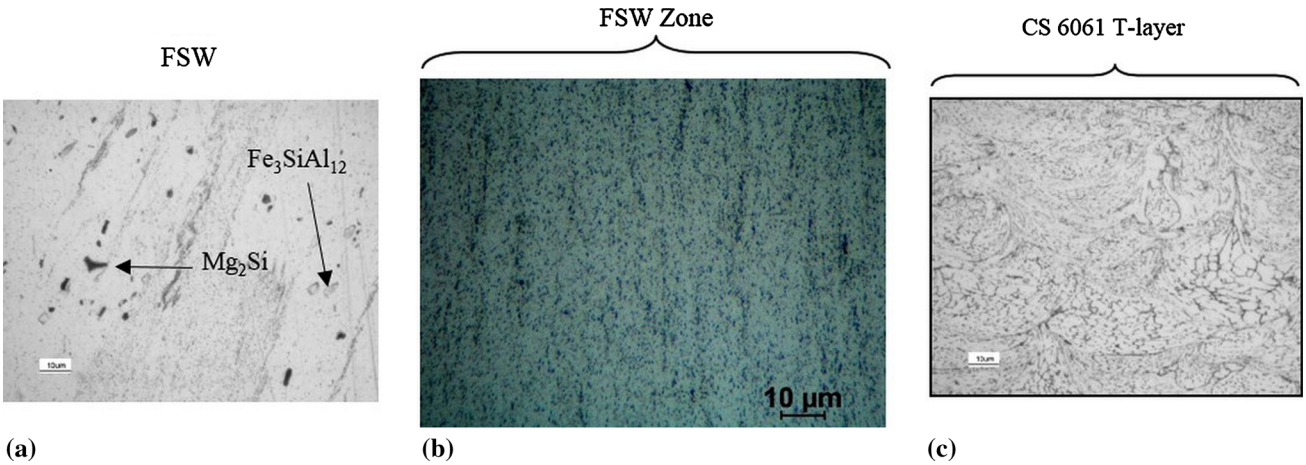

Fig. 15 (a), (b), and (c). Etched optical micrographs of the completed welded joint showing areas identified in Fig. 14 at higher magnifications. Each marker represents 10 μm

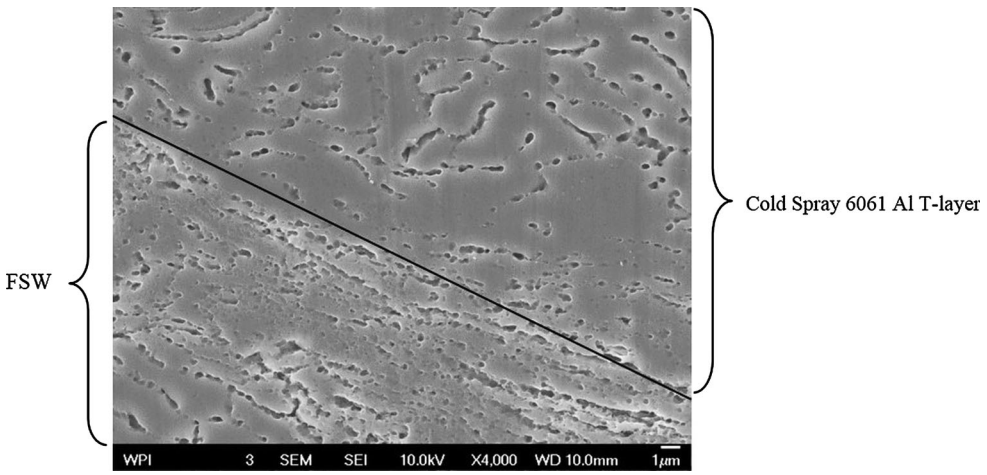

Fig. 16 SEM of the CS 6061 Al T-layer and FSW interface

flow stress of the aluminum is sensitive to temperature, decreasing as temperature increases. During impact of the solid feed stock powder particles, the oxide layers on both the powder and the substrate surface are disrupted and partially removed along with other impurities at the particle substrate interface causing the exposure of highly

reactive ''virgin'' metal and subsequent metallurgical bonding between particle and substrate material (Ref 37). The feedstock powder is in intimate contact with the exposed substrate and forms an adherent metallurgical bond as a result of the severe plastic deformation during particle impact (Ref 28). Therefore, it can be deduced based upon empirical evidence that adiabatic shear, in combination with mechanical interlocking, serves as the predominate bonding mechanism for the cold spray 6061 Al transitional layer.

The important aspect of this study was to develop a cold spray transitional layer that could withstand the frictional forces and contact pressures exerted during the FSW process. Figure 16 depicts the microstructure representative of the interfacial region between the FSW and the CS 6061 Al T-layer. There is complete mechanical mixing between the wrought 6061 Al and the CS 6061 Al T-layer, and the bond was free from any inherent material defects such as porosity or cracks.

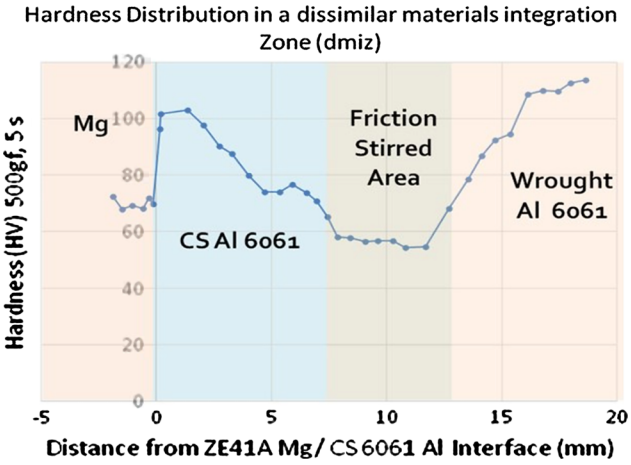

Fig. 17 Microhardness traverse across the Mg substrate, CS/FSW nugget, and into the wrought 6061

5.9 Microhardness and Nanohardness Testing

Two sets of Vicker's microhardness measurements were performed on samples of the completed welded joint. Measurements were taken across all of the various regions of interest, as shown in Fig. 17. A microhardness traverse (collected from a substrate/coating cross-section) was conducted where measurements were obtained with a fixed separation of 0.3 mm, traveling from the Mg substrate through the Cold Spray T-layer/Mg substrate interface, across the surface of the Cold spray T-layer and through the entire FSW region and into the wrought 6061 Al. The position of the indentation relative to the various regions was measured using optical microscopy in conjunction with image analysis. Vickers hardness testing was performed using a 500 g load. Nanohardness measurements were also taken in the same manner utilizing a Keyence Nanoindenter XP, which yielded 1000 nm depth indentations, using a Berkovich tip. Three test points per location were measured and plotted against the second set of Vickers microhardness measurements, as shown in Fig. 18.

The results show the hardness gradient across the dissimilar materials integration zone (DMIZ), which is that area defined from the interface of the magnesium substrate across the Cold spray T-layer and FSW region and to the interface of the wrought 6061 Al. The hardness across the FSW region was lower than both that of the cold spray 6061 Al, as well as the wrought 6061 Al due to mechanical mixing of the materials being FSW (Ref 38, 39). During FSW, overaging and coarsening of strengthening precipitates can reduce the hardness (Ref 40).

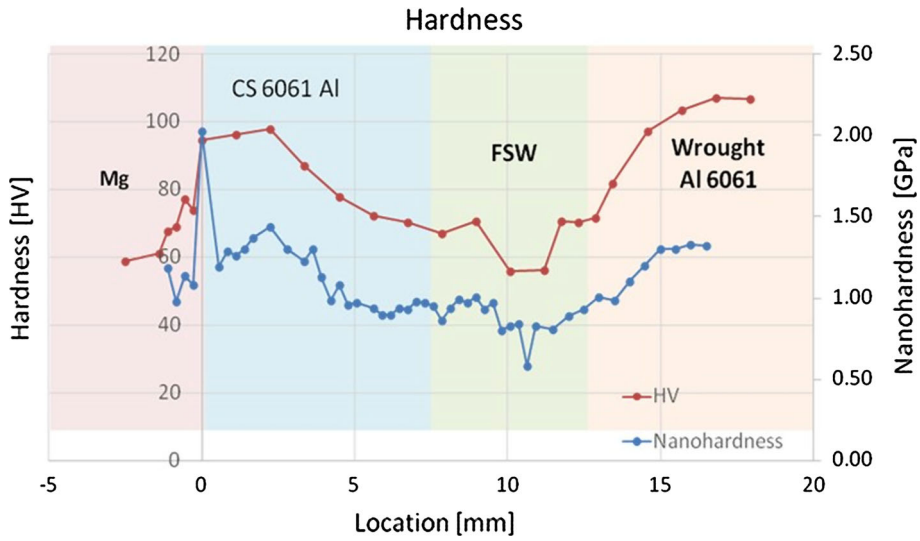

Fig. 18 Microhardness and nanohardness traverse across the Mg substrate, CS/FSW, and the wrought 6061Al

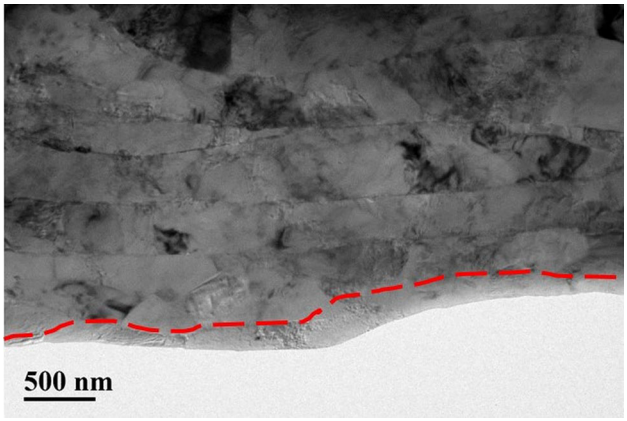

Fig. 19 Formation of pancaked structures at some of the interfaces, as result of SPD

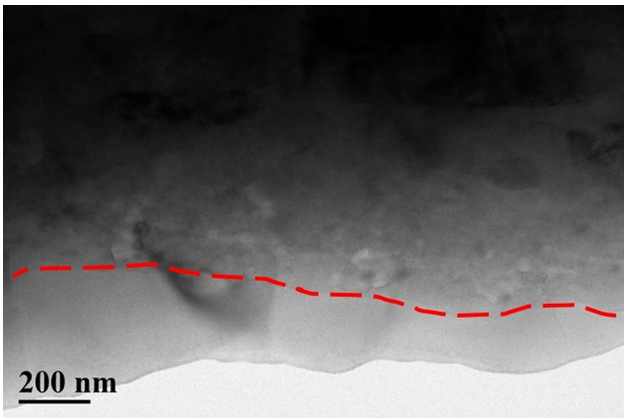

Fig. 20 Formation of UFG structures at other interfaces due to high strain-rate deformation

5.10 Transmission Electron Microscopy Analysis

Transmission Electron Microscopy was performed utilizing a JEM-2100 LaB6 Tem microscope equipped with EDS analysis operating at 200 kV. Thin disks of 3 mm diameter were excised from the cold spray aluminum transitional layer/magnesium substrate such that the interface was aligned in the middle of the final samples, and then polished, dimpled, and ion milled for 5 h. Based on the numerous TEM micrographs, 3 different types of interfaces were characterized in the CS 6061 Al T-layer/ZE41A Mg substrate, as shown in Fig. 19, 20, 21, and 22: interfaces with pancaked structures, interfaces with ultra-fine grained (UFG) structures, and interfaces with fine intermetallic phases.

As observed in Fig. 19, the spherical particles have undergone severe plastic deformation (SPD), become elongated through the cold spray deposition process, and formed pancaked structures at the interface. The significant change in particle morphology during the CSP is due to impact with the underlying substrate and subsequently impacting powder particles. During CS processing, particles experienced enough deformation to remove the surface oxide to expose fresh material. Thermal softening due to the presence of SPD can enhance particle deformation and interlocking of adjacent particles resulting in the intimate contact at the interface and consequently pancaked structures in the deposited material. However, the deformation for these particles was not enough to cause recrystallization or intermetallic phase formation.

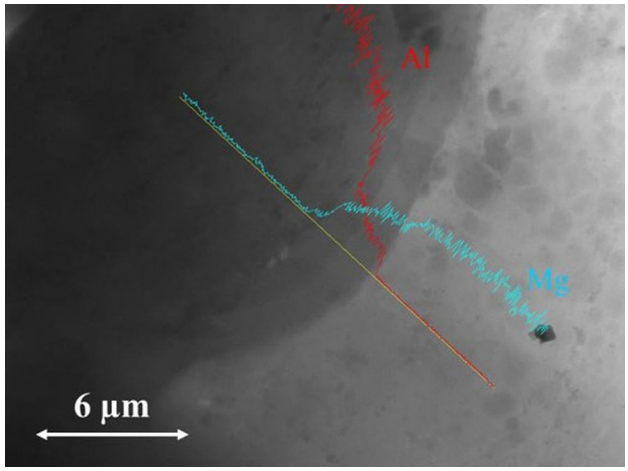

Fig. 21 TEM micrograph showing the presence of intermetallic phases at the interface

It is evident in Fig. 20 that some of the particles have experienced sufficient deformation and heat during the impact that they have completely recrystallized at the interface, resulting in the formation of an UFG structure. This is an evidence for the occurrence of continuous dynamic decrystallization (CDRX) and conversion of the low-angle grain boundaries (LAGBs) to high-angle grain boundaries (HAGBs).

Finally, several other interfaces were also characterized with some fine intermetallic phases. As can be seen in Fig. 21, some of the particles have experienced enough heat during the impact that they have developed a region with different composition, i.e., a mix of Al and Mg elements, at the interface between the cold spray transitional layer and the substrate. Based on all the TEM images, the thickness of this region varies from couple hundred nanometers to ~3 microns. In addition, from the inspection of Fig. 21, this region, which has a different composition, can be divided into two distinct zones with two totally different compositions. This feature is more evident is Fig. 22. As can be seen Fig. 22(a), which is a scanning TEM image (STEM), the region close to the Al coating is heavier as it shows up with darker color than the region close to the substrate, and there is a boundary between these regions, which can be observed in Fig. 22(b).

To study the composition of these regions, the phase diagram between Al and Mg (Fig. 23) shows these binary Al-Mg phases. Upon heating up together during processes like cold spray, the Al-rich phase and the Mg-rich phase can react with each other in the solid state to form intermetallic compounds, such as Al3Mg2 or Al12Mg17,

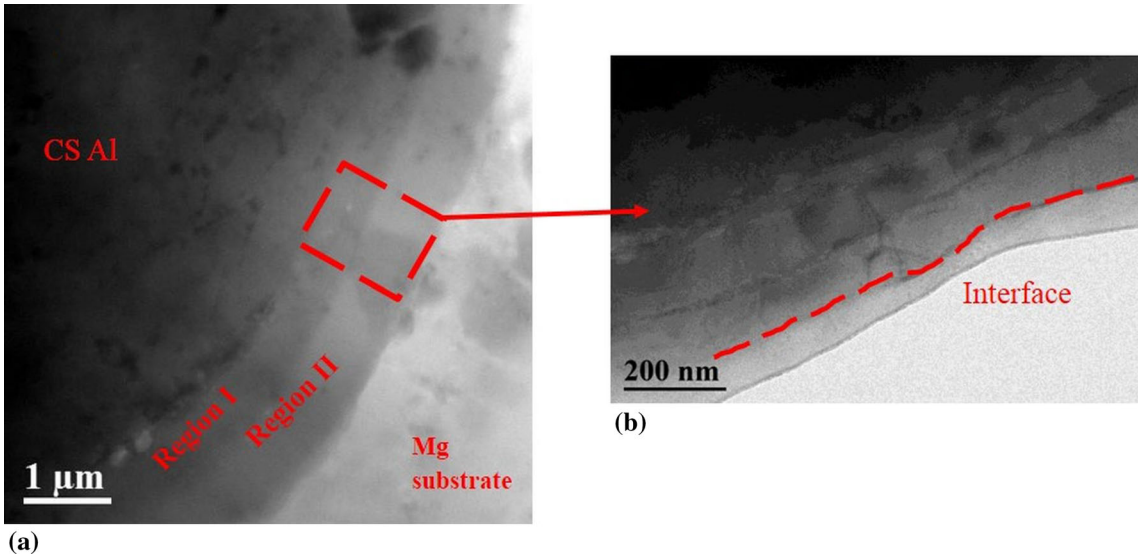

Fig. 22 TEM micrograph from the interfaces with intermetallic phases

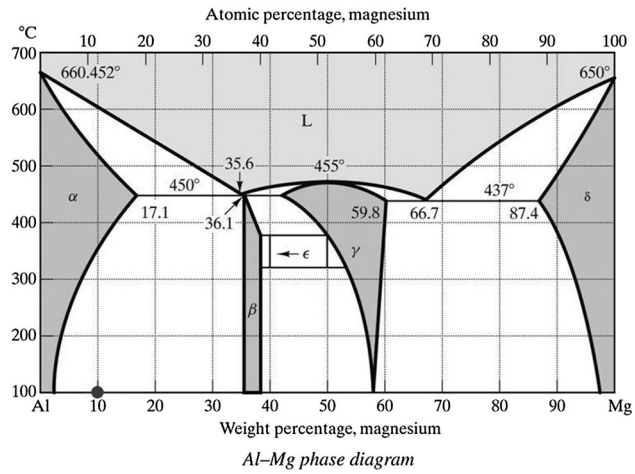

Fig. 23 Al-Mg phase diagram (Ref 41)

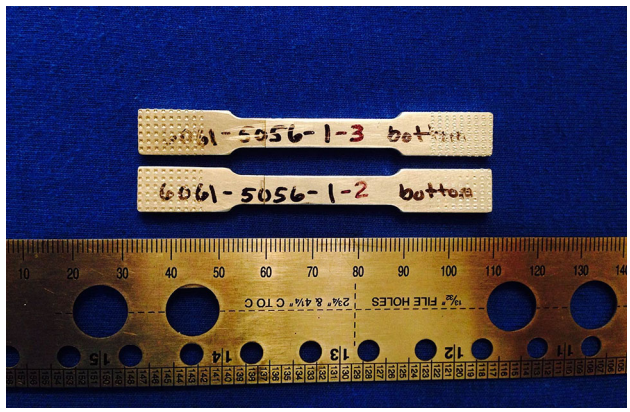

Fig. 24 Flat tensile specimens machined from the completed dissimilar material joint between Cast ZE41A-T5 Mg to Wrought 6061-T6 Al using cold spray 5056 Al as the transitional layer

Table 6 EDS analysis of various regions within TEM of the interface between the CS 6061 Al T-layer and ZE41A Mg substrate

Spectrum	Mg	Al	Remaining elements	Total
Al coating	1.59	98.20	0.21	100.00
Region I	39.91	50.66	9.43	100.00
Region II	52.98	32.59	14.42	100.00
Mg substrate	93.63	1.47	4.90	100.00

depending on the local composition that are stable at room temperature.

The EDS detector on TEM microscope was used to analyze the exact composition of these regions. The results are presented in Table 6. As was expected, region I has more Al with about 40% Mg and region II contains more Mg (~53% Mg). These results are in full agreement with the literature and represent (39.23-39.27 at.% Mg) close to the Al deposition, and phase (51.97-55.41 at.% Mg) close to the Mg substrate.

It was deduced that having these three types of structures at the interface originated from particle size distribution for the as-received 6061 Al powder and their corresponding CIV during cold spraying. CIV is an important factor for the amount of deformation that the particles experience upon their impact to the substrate.

5.11 Tensile Testing of Joined Cast ZE41A-T5 Mg to Wrought 6061-T6 Al

A series of tensile tests were carried out on completed joints (see Fig. 3 for the joint design) in accordance with ASTM E8, using a strain rate of 0.05 in/min at room temperature and ~50% relative humidity. A total of (5)

Table 7 Tension testing of joined cast ZE41A-T5 Mg to Wrought 6061-T6 Al using 6061 Al as the T-layer

SPEC #	UTS, MPa	%ep @ failure
6061 Al-T layer		
1	130	0.3
2	164	0.4
3	164	0.5
4	160	0.3
5	132	0.2
AVG.	150	0.3

Table 8 Tension testing of joined cast ZE41A-T5 Mg to Wrought 6061-T6 Al using 5056 Al as the T-Layer

SPEC #	UTS, MPa	%ep @ failure, %
5056 Al -T layer		
1	198	0.2
2	194	0.3
3	197	0.2
4	194	0.7
5	181	0.3
AVG.	193	0.3

flat tensile specimens were machined from the actual joined cast ZE41A-T5 Mg to wrought 6061-T6 Al using a 6061 Al cold spray transitional layer and the other (5) tensile specimens were machined from the actual joined cast ZE41A-T5 Mg to wrought 6061-T6 Al using a 5056 Al cold spray transitional layer (Fig. 24). All tensile specimens were approximately 10 mm wide × 76 mm long × 3 mm in thickness. Only the UTS and percent elongation (%EL) were recorded because there were three areas with dissimilar materials joined together, and additional measurements of YS and the modulus of elasticity would be combinations of these different materials, making these measurements questionable. Typically specifications require the UTS, and the joint strength is usually required to exceed the minimum specified UTS of the weakest parent metal, which in this study would be the ZE41A-T5 Magnesium at about 205 MPa (Ref 29).

The data in Table 7 show that the average value of UTS of the completed joints using 6061 Al cold spray for the transitional layer was lower than those incorporating 5056 Al cold spray for the transitional layer, shown in Table 8. As explained previously in section "*Tension Testing of the 6061 Al Cold Spray Material Comprising the Transitional Layer*," and reported in Table 5, the UTS of the cold spray 6061 Al T-layer was 315 MPa, as opposed to that of the 5056 Al cold spray T-layer, which was significantly higher at 400 MPa. However, it is the integrity of the bond between the cold spray T-layer and the ZE41A Mg substrate that is the limiting factor.

6. Discussion

The concept of utilizing the CSP to join dissimilar materials has been demonstrated in this study, which is the main focus of this paper. A cold spray transitional layer of aluminum (either 6061 or 5056) was deposited onto the edge of cast ZE41A-T5 magnesium that was later joined to wrought 6061-T6 Al by the FSW process. Materials' characterization showed the absence of a coarse intermetallic layer being formed at the FSW region. This combination of materials was chosen because of their widespread applicability across several sectors of industry and throughout the US Department of Defense. The novel aspect of the concept to join dissimilar materials by the CSP is the cold spray T-layer, which is the key element to enable the joining of dissimilar materials that, prior to this work, had never been achieved with any degree of structural integrity because of numerous limitations, of which the primary is the high thermal input associated with conventional welding techniques and the subsequent formation of these deleterious intermetallics. Additionally, other factors that prohibit the use of conventional welding techniques include the formation of tensile residual stresses due to the contraction of a weld melt pool and restrictions on the types of materials that can be joined because of chemical incompatibility.

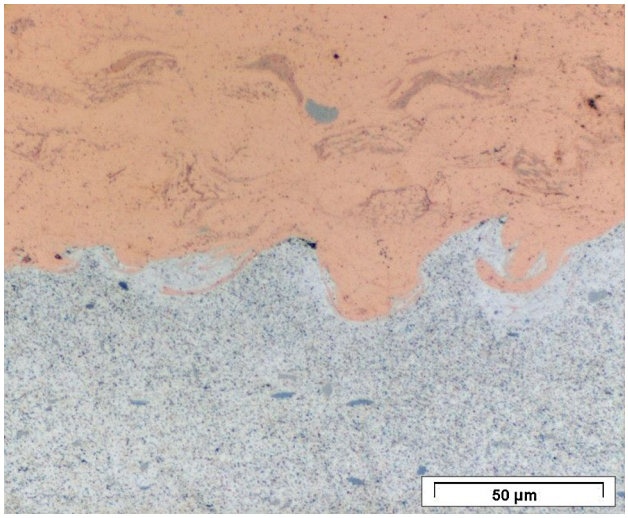

Fig. 25 Copper deposited onto 6061-T6 Al by the cold spray process showing mechanical mixing

Liu et el conducted a review of dissimilar welding techniques for magnesium alloys to aluminum alloys in 2014 and have also reported that the formations of Mg_2Al_3 and $Mg_{17}Al_{12}$ IMCs are inevitable in the dissimilar Al/Mg joints under all conditions of the welding (Ref 42). It is important to point out that Liu et el identified three primary approaches in an attempt to reduce or eliminate the formation of intermetallic compounds (IMC's) specifically (1) using a solid state process, (2) improving IMC variety and distribution, and (3) reducing reaction and energy but even though the IMC reaction layer could be significantly reduced due to the low welding temperature, the formation of brittle Al-Mg IMCs could not be completely avoided (Ref 42). In this study and that of Somasekharan and Murr (Ref 11), the microstructural characteristics associated with FSW were similar, in that the swirled

pattern of intercalated microstructure with vortexes were observed but the heat generated by the FSW of the CSP samples did not penetrate into the Mg, and therefore, no intermetallics were formed. The cold spray material served as the transitional material allowing the two dissimilar metals to be joined without the formation of undesirable coarse intermetallics or other undesirable microstructural features, such as HAZs or the formation of an as-cast structure. The most significant grain refinement was observed within the cold spray transitional layer. During impact of the solid feed stock powder particles, the oxide layers on both the powder and the substrate surface are disrupted and partially removed along with other impurities at the particle substrate interface causing the exposure of highly reactive ''virgin'' metal and subsequent metallurgical bonding between particle and substrate material. (Ref 37) Adiabatic shear, in combination with mechanical interlocking, serves as the predominate bonding mechanism for the cold spray Al transitional layer, although recent studies also point toward diffusive heat conduction (Ref 43). Figure 25 substantiates this with a more vivid micrograph showing copper deposited onto 6061 Al by the cold spray process. The contrast between the two materials makes it easier to distinguish the high strain-rate mechanical mixing. The hardness across the FSW region was lower than both that of the cold spray 6061 Al, as well as the wrought 6061 Al due to mechanical mixing of the materials being FSW (Ref 38, 39). During FSW, overaging and coarsening of strengthening precipitates reduced the hardness (Ref 40).

The cold spray T-layer was examined by optical and electron microscopy, which confirmed the absence of a coarse intermetallic layer and/or coarse IMCs. Observations of the FSW weld zone revealed the unique dissimilar weld flow characteristics showing that the cold spray material had sufficient structural integrity allowing it to withstand the mechanical force and thermal input induced by the FSW process. Shear strength testing of the 6061 Al cold spray transitional material deposited onto the ZE41A Mg showed that the interface was equal to or stronger than the magnesium substrate in shear. Analysis of the UTS of both the cold spray 6061 Al and 5056 Al bulk materials used as the transitional layers revealed a greater UTS and ductility than the ZE41A Mg to which they were deposited onto. However, when the samples of joined cast ZE41A-T5 Mg to wrought 6061-T6 Al were produced, the adhesion of the CS 6061 T-layer to the base magnesium were not as high and had to be improved to reach that achieved by the 5056 Al cold spray T-layer. The differences in adhesion were attributed to differences in the robotic path planning that was performed to deposit the cold spray transitional layers. A more sophisticated program was used for the deposition of the 5056 Al cold spray. The reason for this was the fact that a separate project was being conducted to develop advanced robotic programming to improve cold spray adhesive strength, and these samples were produced toward the end of the subject study.

7. Conclusions

- The Cold Spray 6061 Al transitional layer had a higher shear strength (141 MPa) than the cast ZE41A-T5 Mg (122 MPa) and the CS 6061 Al T-layer had exceptional UTS (315 MPa) and elongation (5.2%), higher than that of the cast ZE41A-T5 Mg and approximately the same as wrought 6061-T6 Al. The CS 5056 Al had a UTS of (400 MPa) and an elongation of (15%).
- A typical hardness gradient was observed across the DMIZ. The hardness across the FSW nugget was lower than both that of the cold spray 6061 Al, as well as the wrought 6061 Al due to the heat generated during the FSWP. The temperature increases due to FSW offset any hardening gained from any grain refinement.
- The FSW zone between the wrought 6061 Al and the CSP transitional layer revealed evidence of an intercalated microstructure with vortexes as a result of mechanical mixing of the two metals, typical of FSW, demonstrating that the cold spray transitional layer was conducive to the FSW process.
- SEM analysis of the 6061 Al T-layer showed evidence of recrystallization of the highly deformed powder particles from high strain-rate adiabatic shear. The CS T-layer near the substrate interface had good deposition quality with no extensive porosity, triple junction voids, or lack of bonding between powder particles.
- TEM analysis revealed continuous dynamic recrystallization (CDRX) and conversion of the LAGBs to HAGBs. There was no evidence of the formation of coarse deleterious intermetallic compounds or layer formed but fine intermetallic phases ranging in size from a few hundred nanometers to ~3 microns were found and deduced to be the result of localized heating through the transfer of kinetic energy from impacting particles during cold spray.
- Tensile testing of the completed welded joint showed high UTS, but the ductility was low $<1\%$ and needs improvement.
- The results of this work demonstrate a practical method to join dissimilar materials, specifically, wrought 6061-T6 Al alloy to cast ZE41A-T5 Mg, by a combination of the CSP and FSW.

Acknowledgments

This work was funded by the National Science Foundation through the South Dakota School of Mines and Technology. A joint patent application was filed through the Army Research Laboratory (ARL 13-44, Application #61930613).

References

1. L.M. Zhao and Z.D. Zhang, Effect of Zn Alloy Interlayer on Interface Microstructure and Strength of Diffusion-Bonded Mg-Al Joints, *Scr. Mater.*, 2008, **58**, p 283-286
2. P. Liu, Y.J. Li, H.R. Geng, and J. Wang, *Mater. Lett.*, 2005, **59**, p 2001
3. A. Kostka, R.S. Coelho, J. Santos, and A.R. Pyzalla, Microstructure of Friction Stir Welded Aluminium Alloy to Magnesium Alloy, *Scr. Mater.*, 2009, **60**(11), p 953-956
4. A. Ben-Artzy, A. Sternb, N. Frage, V. Shribman, and O. Sadot, Wave Formation Mechanism in Magnetic Pulse Welding, *Int. J. Impact Eng.*, 2010, **37**, p 397-404
5. L. Liu and H. Wang, Microstructure and Properties Analysis of Laser Welding and Laser Weld Bonding Mg to Al Joints, *Metall. Mater. Trans. A.*, 2011, **42**(4), p 1044-1050
6. Rattana Borrisutthekul, Yukio Miyashita, and Yoshiharu Mutoh, Dissimilar Material Laser Welding between Magnesium Alloy AZ31B and Aluminum Alloy A5052-O, *Sci. Technol. Adv. Mater.*, 2005, **6**, p 199-204
7. Peng Liu, Yajiang Li, Haoran Geng, and Juan Wang, Microstructure Characteristics in *TIG* Welded Joint of Mg/Al Dissimilar Materials, *Mater. Lett.*, 2007, **61**, p 1288-1291
8. A. Ben-Artzy, A. Munitz, G. Kohn, B. Bronfin, and A. Shtechman, *TMS Meeting 2002*, *Magnesium Technology*, 2002, p 295
9. O. Tomiharu, *J. Light. Metal. Weld. Const*, 2004, **42**, p 2
10. J. Shang, K. Wang, Q. Zhou, D. Zhang, J. Huang, and G. Li, Microstructure Characteristics and Mechanical Properties of Cold Metal Transfer Welding Mg/Al Dissimilar Metals, *Mater. Des.*, 2011, **34**, p 559
11. A.C. Somasekharan and L.E. Murr, Microstructures in Friction-Stir Welded Dissimilar Mg Alloys and Mg Alloys to 6061-T6 Aluminum Alloy, *Mater. Charact.*, 2004, **52**, p 49-64
12. C. Toma, E. Cicala, P. Sallamand, and D. Grevey, CMT Joining of Aluminum Magnesium Alloys in a Statistical Experiment, *Metal*, 2012, Brno, **5**, p 23-25
13. A. Papyrin, Cold Spray Technology, *Adv. Mater. Process.*, 2001, **159**, p 49–51
14. T.H. Van Steenkiste, Kinetic Spray Coatings, *Surf Coat Tech.*, 1999, **111**, p 62
15. T. Stoltenhoff, H. Kreve, and H. Richter, An Analysis of the Cold Spray Process and its Coatings, *J. Therm. Spray Technol.*, 2002, **11**(4), p 542
16. R. Dykhuisen and M. Smith, Gas Dynamic Principles of Cold Spray, *J. Therm. Spray Technol.*, 1998, **7**(2), p 205
17. V.F. Kosarev, S.V. Klinkov, A.P. Alkhimov, A.N. Papyrin, and 2, On Some Aspects of Gas Dynamic Principles of Cold Spray Process, *J. Therm. Spray Technol.*, 2003, **12**, p 265
18. M. Gujicic, C.L. Zhao, C. Tong, W.S. DeRosset, and D. Helfritch, Analysis of the Impact Velocity of Powder Particles in the Cold-Gas Dynamic-Spray Process, *Mater. Sci. Eng. A*, 2004, **368**, p 222
19. R.C. Dykhuizen, M.F. Smith, D.L. Gilmore, R.A. Neiser, X. Jiang, and S. Sampath, Impact of High Velocity Cold Spray Particles, *J. Therm. Spray Technol.*, 1999, **8**(4), p 559
20. M. Grujicic, J.R. Saylor, D.E. Beasley, W.S. Derosset, and D. Helfritch, Computational Analysis of the Interfacial Bonding between Feed-Powder Particles and the Substrate in the Cold-Gas Dynamic-Spray Process, *Appl. Surf. Sci.*, 2003, **219**, p 211
21. V. Champagne, Ed., *The Cold Spray Materials Deposition Process: Fundamentals and Applications*, Woodhead Publishing Limited, Abington Hall, Abington, 2007, p 57
22. M.P. Walsh, *Plat. Met. Rev.*, 2000, **44**, p 22-30
23. S.M. Bernard, J.M. Samet, A. Grambsch, K.L. Ebi, and I. Romieu, *Environ. Health Perspect.*, 2001, **109**, p 199-209
24. A. Buxton and I. Norris, Dissimilar materials…Novel Solutions to Joining the Unjoinable, TWI Bulletin, 2008
25. J. Gould, Automakers Look to Solid State Welding of Dissimilar Metals. Fastening/Joining/Assembly Supplement
26. R. Huang and H. Fukanuma, Study of the Influence of Particle Velocity on Adhesive Strength of Cold Spray Deposits, *J. Therm. Spray*, 2012, **548**(3-4), p 541-549
27. MIL-J-24445A, Joint, Bimetallic Bonded, Aluminum to Steel, Commander, Naval Ship Engineering Center, SEC 6124, Department of Navy, Washington, 20362, http://everyspec.com/MIL-SPECS/MIL-SPECS-MIL-J/MIL-J-24445A_11054/. Accessed June 2014
28. R. Maev, V. Leshchynsky, and A. Papyrin, Structure Formation of Ni-based Composite Coatings During Low Pressure Gas Dynamic Spraying. *Proceedings of the 2006 ITSC*, ASM, Seattle, 2006
29. MATWEB. Chemical Composition of ZE41A Magnesium
30. W. Kasprzak et al., Correlating Hardness Retention and Phase Transformations of Al and Mg Cast Alloys for Aerospace Applications, *J. Mater. Eng. Perform.*, 2015, **24**(3), p 1365-1378
31. Y. Riddle, L. Barber, Y. Riddle, L. Barber, and M. Makhlouf, Characterization of Mg Alloy Solidification and As-Cast Microstructure, Magnesium Technology, TMS, 2004, p 203-208
32. I.J. Polmear, Light Alloys-Metallurgy of the Light Metals, *Metallurgy and Materials Science Series*, 3rd ed., Butterworth-Heinemann, Burlington, 1995,
33. M.R. Rockni, C.A. Widener, and V.K. Champagne, Microstructural Evolution of 6061 Al Gas-Atomized Powder and High-Pressure Cold-Sprayed Deposition'', *J. Therm. Spray*, 2013, doi:10.1007/s11666-013-0049-y
34. G.E. Dieter, *Mechanical Metallurgy*, McGraw-Hill Series in Materials Science and Engineering McGraw-Hill, Singapore, 2001
35. V.K. Champagne, *The Cold Spray Materials Deposition Process: Fundamentals and Applications*, Woodhead Publishing Limited, Cambridge, 2007
36. Mechanical Properties of 6061-T6 Aluminum. ASM MATWEB
37. T. Stoltenhoff and F. Zimmermann, LOXPlate® Coatings for Aluminum Aerospace Components Exposed to High Dynamic Stresses'', Praxair Surface Technologies GmbH, Ratingen
38. J.A. Schneider and A.C. Nunes, Thermo-mechanical processing in friction stir welds, *Proceedings of symposium sponsored by the shaping and forming committee of the materials processing and manufacturing division of the minerals, metals, and materials society (TMS)*, Warrendale, TMS, 2003, p 43-51
39. P.L. Threadgill, Friction-Stir Welding-State of the Art, TWI, Report 678, England, 1999
40. S. Ravikumar et al., Effect of Process Parameters on Mechanical Properties of Friction Stir Welded Dissimilar Materials between AA6061-T651 and AA7075-T651 Alloys, *Int. J. Adv. Mech. Eng.*, 2014, **4**(1), p 101-114
41. A. Lugovskoy, Al-Mg Phase Diagram. al-chemist.info/node/161
42. Liming Liu, Daxin Ren, and Fei Liu, A Review of Dissimilar Welding Techniques for Magnesium Alloys to Aluminum Alloys, *Materials*, 2014, **7**, p 3735-3757. doi:10.3390/ma7053735
43. T. Schmidt et al., From Particle Acceleration to Impact and Bonding in Cold Spray, *J. Therm. Spray Technol.*, 2009, **18**(5-6), p 794